

3-D distribution of flux density and an inference about scalar potential in flux concentration model

著者	Yoshimoto T., Yamada Sotoshi, Bessho Kazuo
journal or publication title	IEEE Transactions on Maggetics
volume	23
number	5
page range	3041-3043
year	1987-09-01
URL	http://hdl.handle.net/2297/48315

doi: 10.1109/TMAG.1987.1065419

3-D DISTRIBUTION OF FLUX DENSITY AND AN INFERENCE ABOUT SCALAR POTENTIAL IN A FLUX CONCENTRATION MODEL

T. YOSHIMOTO, S. YAMADA and K. BESSHO

ABSTRACT

This paper deals with the three dimensional analysis of a flux concentration model with two conducting plates placed in parallel between a pair of a.c.-excited coils. We have already presented an analysis for the model with a coarse mesh and volumeless plane coils, as well as newly developed iterative 3-D calculation method. [1] The model analyzed this time has total nodes and elements of about twice as those of the model previously calculated.

The flux density distribution is compared with experimental data. Distributions of eddy currents and scalar potentials are also solved. Flux concentration effect in the air-slit and flux reflection effect over a conducting plate are seen more clearly. An inference about the role of scalar potential is obtained from our calculation results.

INTRODUCTION

A review of the literature reveals that the FEM is the most useful tool for analyzing magnetic fields. Two dimensional or axi-symmetrical quasi-3D FEM calculations have been convenient and popular. However, it is also true that the real 3-D analysis is necessary, especially in treating eddy current problems. A flux concentration apparatus which has been investigated at Kanazawa University since 1981 [2], requires a full three dimensional analysis to clarify the function of the apparatus.

Four component three dimensional FEM formulations, given in references [3] or [4], intrinsically lead to large and sparse system matrices, due to four components per node in addition to the 3-D structure. Our calculation method is devised to avoid this difficulty by dividing the total simultaneous equations into four groups and using an iterative method, so that the computer memory for the main system of equations can be reduced to one sixteenth. This memory saving calculation method enables one to treat the models with much finer division.

As for the controversial theme of the role of the scalar potential [5][6][7], we made a conclusion on the basis of the real calculated distribution of the scalar potential in our model. This distribution is also made possible to obtain by the ability of our calculation method to treat large models.

FIELD EQUATIONS AND ITERATIVE ALGORITHM

For a three dimensional, quasi-stationary, eddy current diffusion problem, Maxwell's electromagnetic field equations together with the definition of the magnetic vector potential are stated as follows:

$$\text{rot } \vec{H} = \vec{J}_s + \vec{J}_e \quad (1)$$

$$\text{rot } \vec{E}_e = -j\omega\vec{B} \quad (2)$$

$$\text{div } \vec{B} = 0 \quad (3)$$

$$\text{div } \vec{D} = \rho \quad (4)$$

$$\vec{B} = \mu\vec{H} \quad (5)$$

$$\vec{J}_e = \sigma\vec{E}_e \quad (6)$$

$$\vec{B} = \text{rot } \vec{A} \quad (7)$$

where, \vec{J}_s and \vec{J}_e are the impressed current and the induced eddy current densities respectively. Combining (2) with (7),

$$\vec{E}_e = -j\omega\vec{A} - \text{grad } \phi \quad (8)$$

where, ϕ in (8) is so-called scalar potential, which plays an important role for dynamic problems. By coupling (8) to (6), the eddy current density \vec{J}_e is

$$\vec{J}_e = -j\omega\sigma\vec{A} - \sigma\text{grad } \phi \quad (9)$$

Substituting (9) in (1), one fundamental equation for field analysis follows, assuming constant μ in the x, y, and z directions.

$$\frac{1}{\mu} \nabla(\nabla\vec{A}) - \frac{1}{\mu} \nabla^2\vec{A} = -\sigma(j\omega\vec{A} + \nabla\phi) + \vec{J}_s \quad (10)$$

The fact that eddy currents do not flow out of conducting materials yields following equation.

$$\text{div } \{ \sigma(j\omega\vec{A} + \text{grad } \phi) \} = 0 \quad (11)$$

The above two equations (10) and (11) are the field analysis equations necessary to determine the vector potential and the scalar potential distributions for eddy current diffusion problems.

Now we introduce, from the standpoint of the computer memory, one iterative method to avoid treating the whole system of equations. From (11), the vector potential \vec{A} is replaced as

$$\nabla\vec{A} = -\nabla^2\phi/j\omega \quad (12)$$

Using (12), (10) can be decomposed into three axis-component equations as shown in (13)-(15). Adding (11), the following four equations are obtained:

$$-\frac{1}{\mu} \nabla^2 A_x + j\omega\sigma A_x = J_{sx} - (\sigma\nabla\phi)_x + \frac{1}{j\omega\mu} \frac{\partial}{\partial x} (\nabla^2\phi) \quad (13)$$

$$-\frac{1}{\mu} \nabla^2 A_y + j\omega\sigma A_y = J_{sy} - (\sigma\nabla\phi)_y + \frac{1}{j\omega\mu} \frac{\partial}{\partial y} (\nabla^2\phi) \quad (14)$$

$$-\frac{1}{\mu} \nabla^2 A_z + j\omega\sigma A_z = J_{sz} - (\sigma\nabla\phi)_z + \frac{1}{j\omega\mu} \frac{\partial}{\partial z} (\nabla^2\phi) \quad (15)$$

$$\nabla \cdot (\sigma j\omega(A_x \vec{u}_x + A_y \vec{u}_y + A_z \vec{u}_z) + \sigma\nabla\phi) = 0 \quad (16)$$

The global system matrix obtained by discretization of (13)-(16) will be generally not only large due to the four components, but also sparse due to the introduction of the scalar potential. The structure of the global system matrix is shown in Fig.1(a). The bandwidth is $3M+M$ (equal nearly to $4N$), if the total number of nodes and the bandwidth are assumed to be N and M , respectively, per each component of \vec{A} . To minimize the band matrix, when we rearrange a column vector of variables from

$$\left[A_{x1} \ A_{x2} \ \dots \ A_{xn} \mid A_{y1} \ A_{y2} \ \dots \ A_{yn} \mid A_{z1} \ A_{z2} \ \dots \ A_{zn} \mid \phi_1 \ \phi_2 \ \dots \ \phi_n \right]^T$$

Manuscript received May 16, 1987.

Takeshi Yoshimoto is with the Department of Electrical Engineering, Ishikawa College of Technology, Tsubata, Ishikawa, 929-03 JAPAN. Sotoshi Yamada and Kazuo Bessho are with the Electrical Energy Conversion Laboratory, Kanazawa University, Kodatsuno, Kanazawa, 920 JAPAN.

into the new form

$$\begin{bmatrix} A_{x1} & A_{y1} & A_{z1} & \phi_1 & | & A_{x2} & A_{y2} & A_{z2} & \phi_2 & | & \dots & | & A_{xn} & A_{yn} & A_{zn} & \phi_n \end{bmatrix}^T$$

the bandwidth reduces to 4M, so that the number of elements of the band matrix reduces to 16 NM as shown in Fig.1(b).

The method we propose in this paper is based on the idea that the four groups of equations, (13) through (16), could be regarded as respective sub-systems of equations regarding A_x, A_y, A_z and ϕ , as shown in Fig.1(c). Though iteration process is needed among the four groups, the bandwidth for each system matrix will be M and the number of elements for each band matrix will be NM. This memory saving of 1/16 is very effective in the circumstance that the general time sharing system of the large-sized computer provides a certain limited region to an individual user. In addition, it also enables us to use the direct calculation method such as Gauss elimination.

The calculation algorithm is: In the first iteration, by giving an arbitrary initial value to $\sigma \nabla \phi$, A_x, A_y, A_z in (13)-(15) are solved and those values are put into (16) for obtaining next values of $\sigma \nabla \phi$. The new values are used again to calculate (13)-(15) in the second iteration. In this way final converged values of A_x, A_y, A_z and ϕ can be obtained. Under-relaxation method is used for correction of ϕ .

FLUX CONCENTRATION MODEL

A flux concentration apparatus utilizing eddy currents is now under investigation at Kanazawa University for the purpose of producing a state of high flux density. Its fundamental model shown in Fig.2 is analyzed. The model configuration is shown in Fig.3. Two conducting plates are placed in parallel with a small slit between them. Eddy currents induced in the

two conducting plates by a.c.-excitation strengthen the flux in the air-slit. The two conducting plates are assumed to be non-magnetic. Using 3-D symmetry, one eighth of the whole region is discretized by using first-order triangular prisms, whose shape functions are in the reference [8]. Neumann condition is imposed on the outer boundary surface with zero vector potential along z-axis.

As for the boundary condition of the scalar potential, zero values are set along the line E-F where eddy currents flow perpendicularly to, for the purpose of conforming the calculated eddy currents with the real flow of eddy currents. Frequency of the impressed current is 60 Hz, the conductivity of the copper plate 8.62×10^7 S/m, the width of the slit 10 mm, and the ampere turn of the excitation coil 1.2 AT/mm^2 .

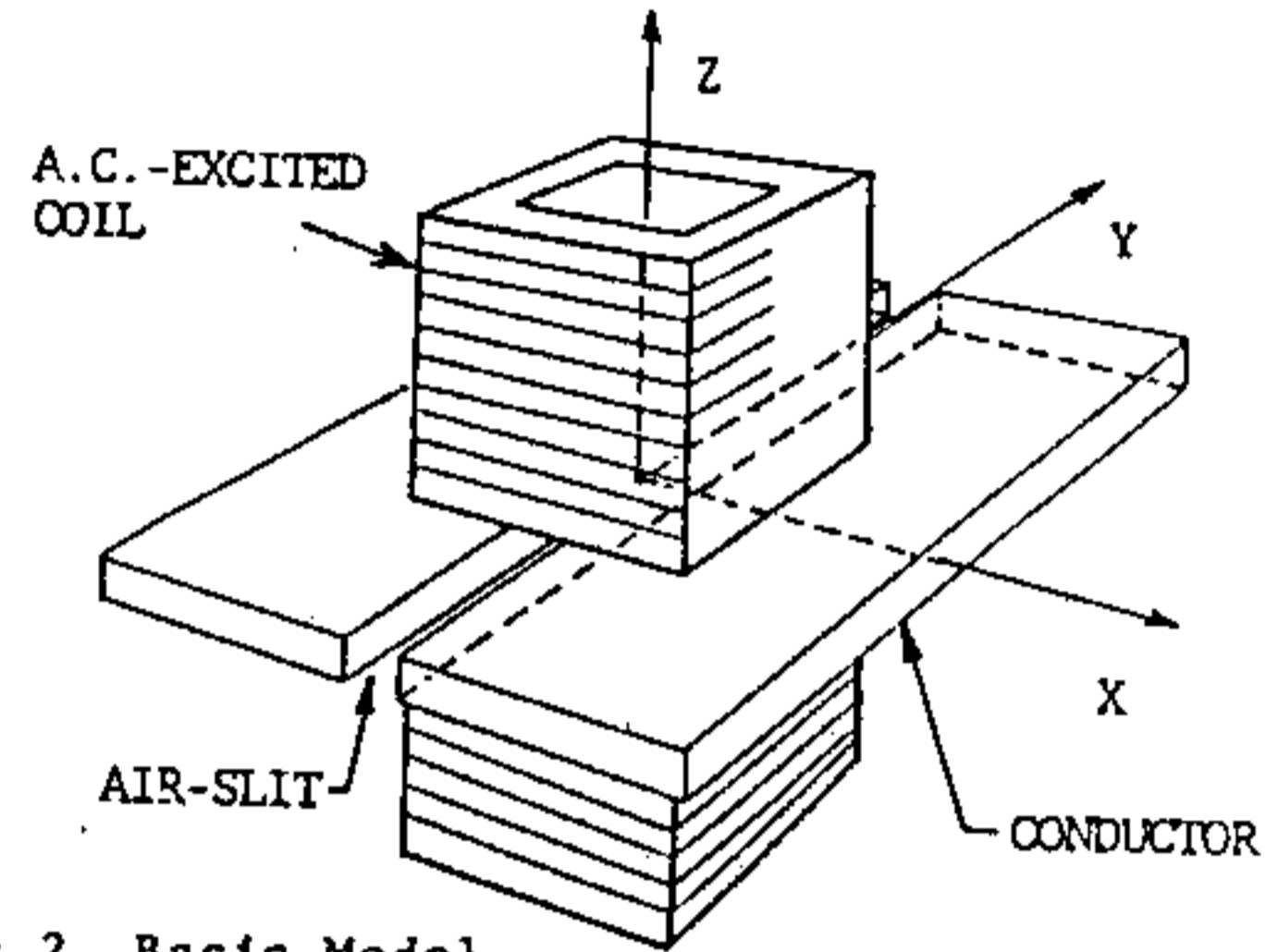
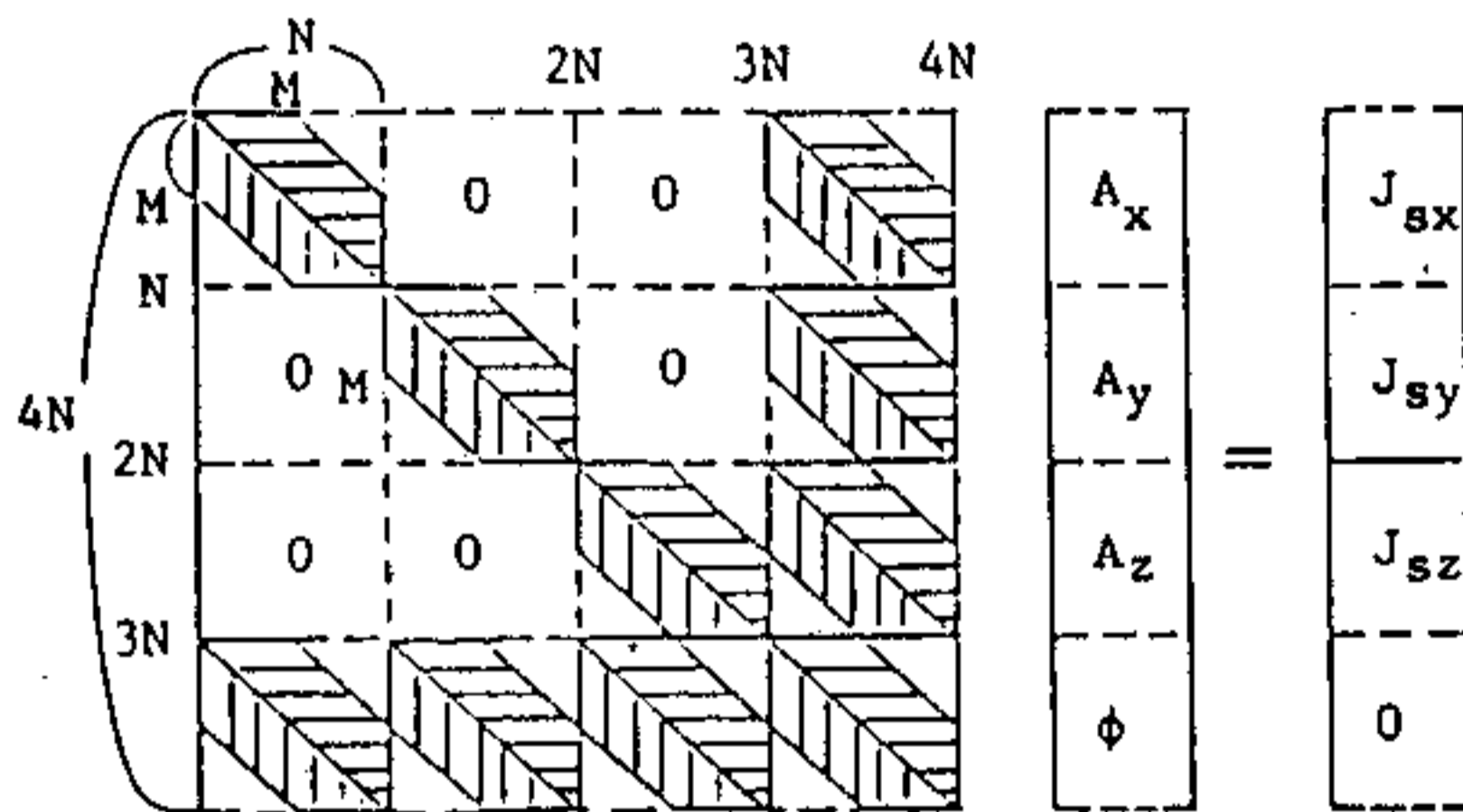
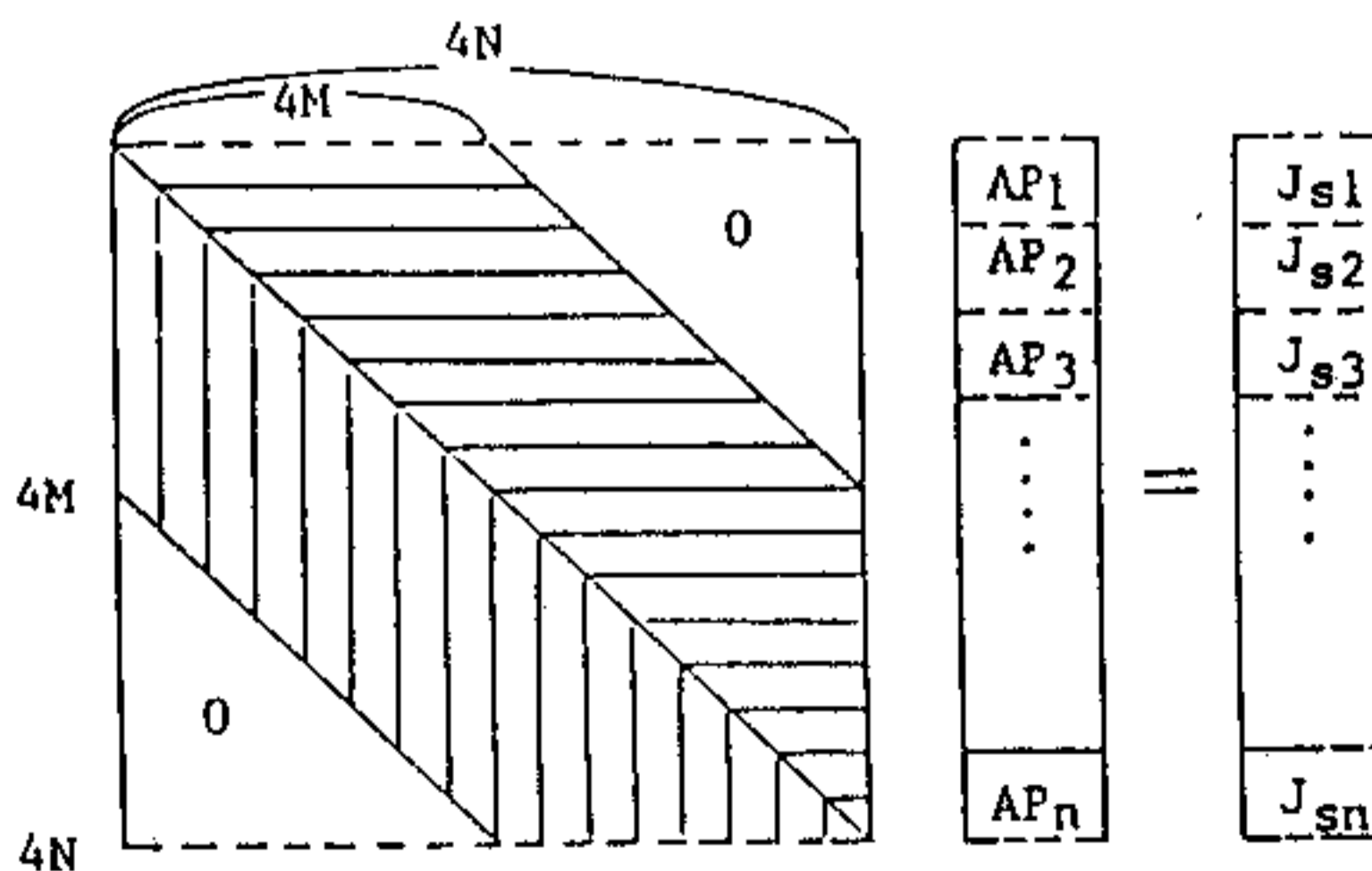


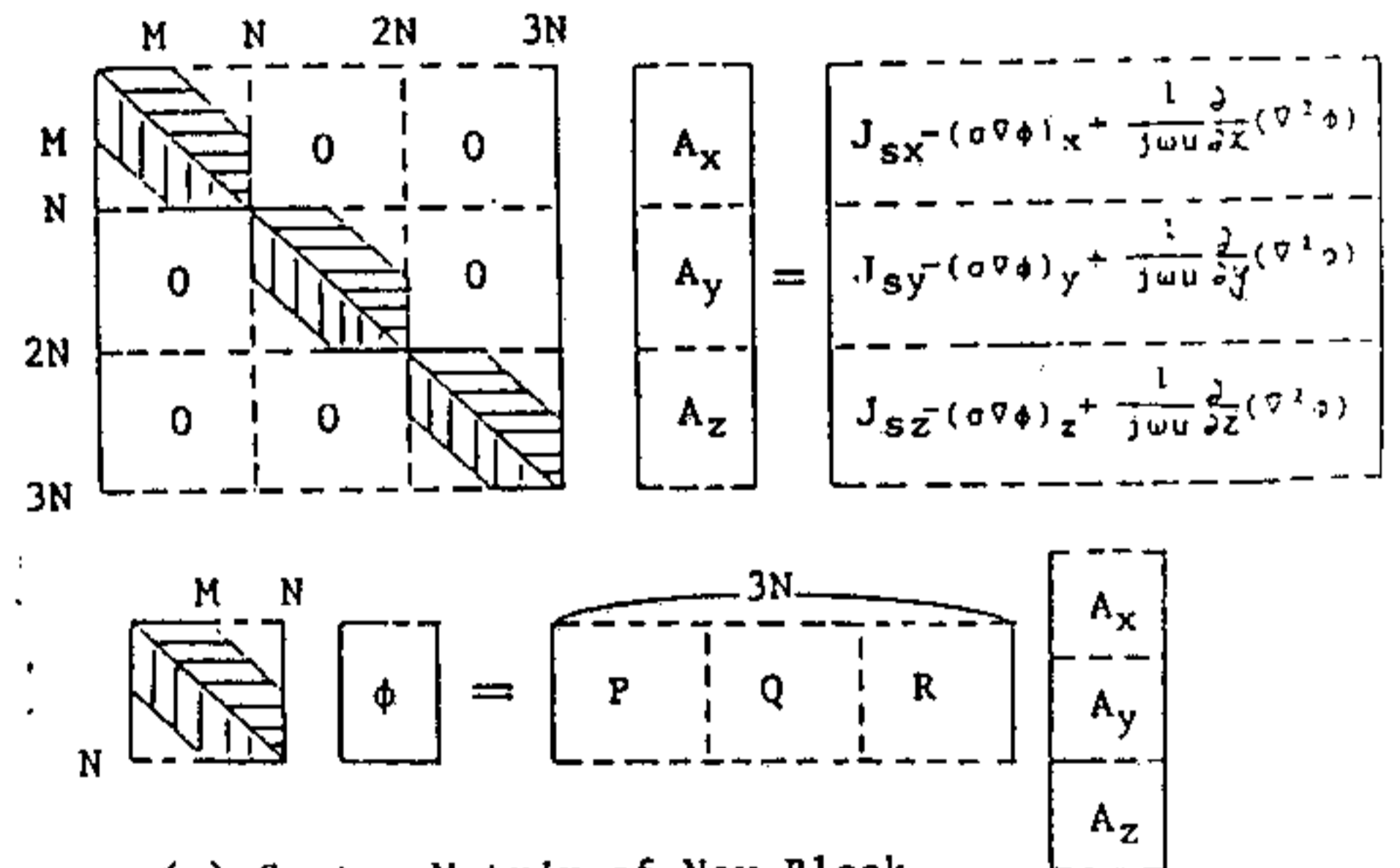
Fig.2 Basic Model of Flux Concentration Apparatus



(a) Global System Matrix



(b) System Matrix with Optimum Band Width



(c) System Matrix of New Block Iteration Method

$$A_x = [A_{x1} \ A_{x2} \ A_{x3} \ \dots \ A_{xn}]^T \quad J_{sx} = [J_{sx1} \ J_{sx2} \ \dots \ J_{sxn}]^T$$

$$A_y = [A_{y1} \ A_{y2} \ A_{y3} \ \dots \ A_{yn}]^T \quad J_{sy} = [J_{sy1} \ J_{sy2} \ \dots \ J_{syn}]^T$$

$$A_z = [A_{z1} \ A_{z2} \ A_{z3} \ \dots \ A_{zn}]^T \quad J_{sz} = [J_{sz1} \ J_{sz2} \ \dots \ J_{szn}]^T$$

$$\phi = [\phi_1 \ \phi_2 \ \phi_3 \ \dots \ \phi_n]^T$$

$$AP_1 = [A_{x1} \ A_{y1} \ A_{z1} \ \phi_1]^T \quad J_{s1} = [J_{sx1} \ J_{sy1} \ J_{sz1} \ 0]^T$$

$$AP_2 = [A_{x2} \ A_{y2} \ A_{z2} \ \phi_2]^T \quad J_{s2} = [J_{sx2} \ J_{sy2} \ J_{sz2} \ 0]^T$$

$$\vdots \quad \vdots$$

$$AP_n = [A_{xn} \ A_{yn} \ A_{zn} \ \phi_n]^T \quad J_{sn} = [J_{sxn} \ J_{syn} \ J_{szn} \ 0]^T$$

Fig.1 Matrix Structure

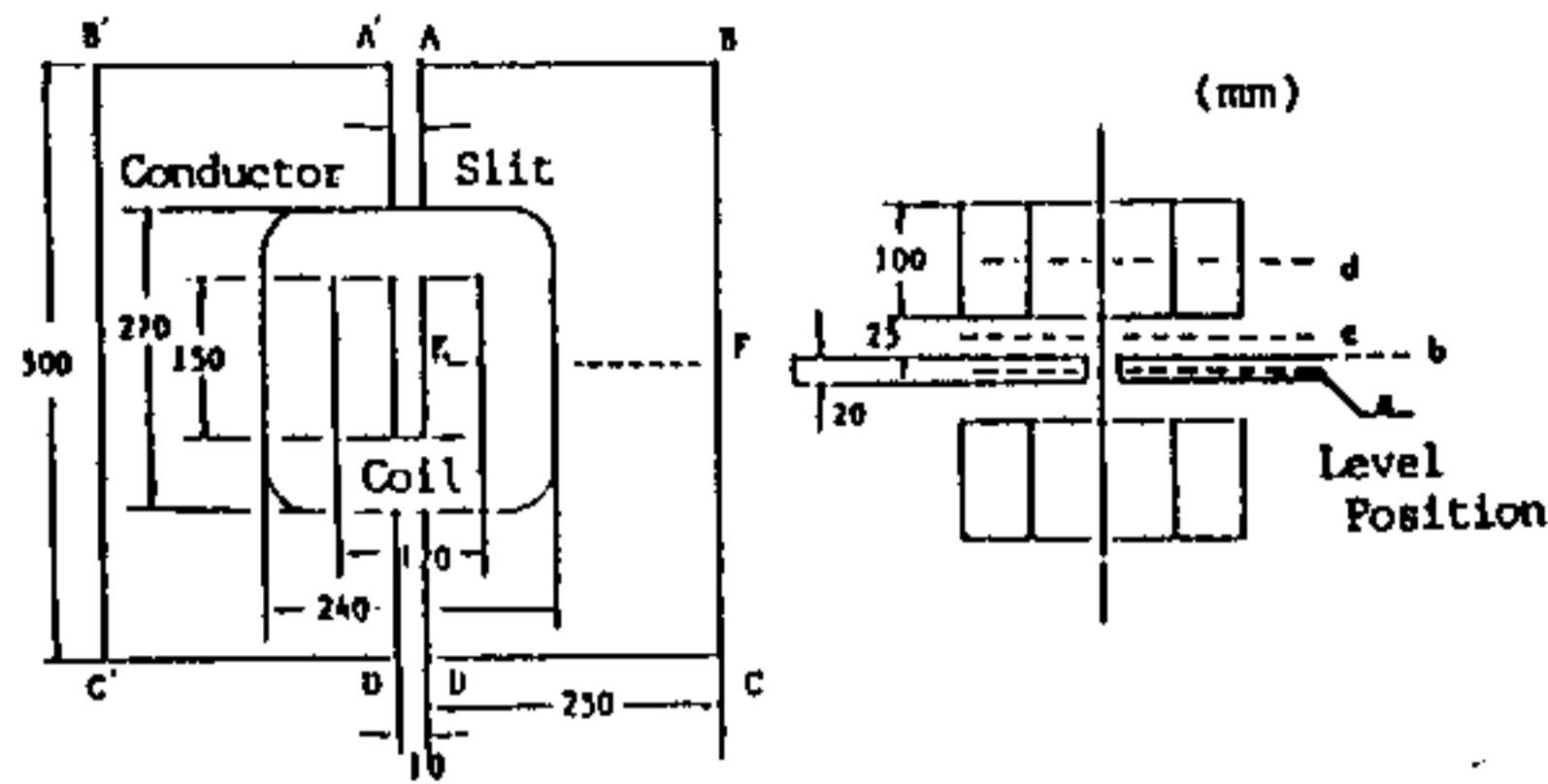


Fig.3 Model Configuration

Calculated distributions of flux density for the applied current of 60 Hz are shown in Fig.4. The flux distribution along the air-slit is shown in the figure (a) for Y-Z plane, while the flux distribution across the plate is shown in the figure (b) for X-Z plane. These figures demonstrate that the flux is concentrated in the air-slit and reflected on the plate surface.

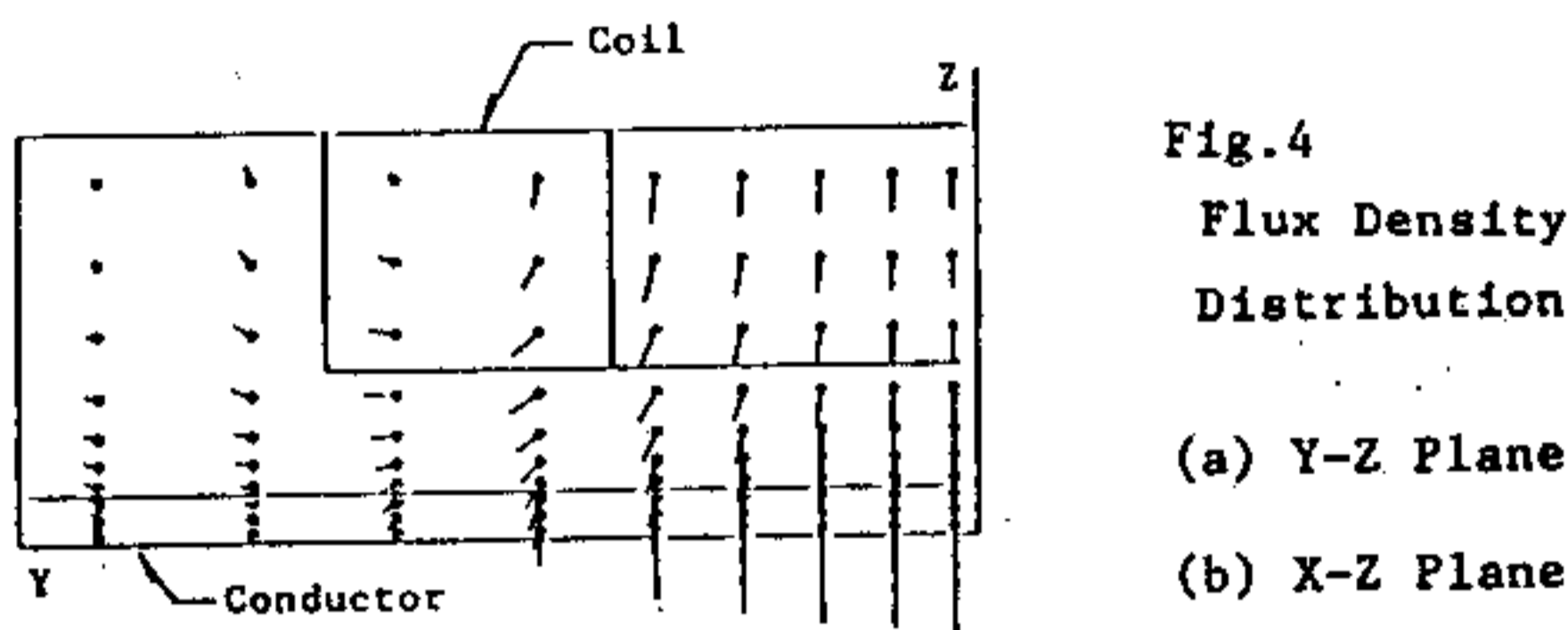
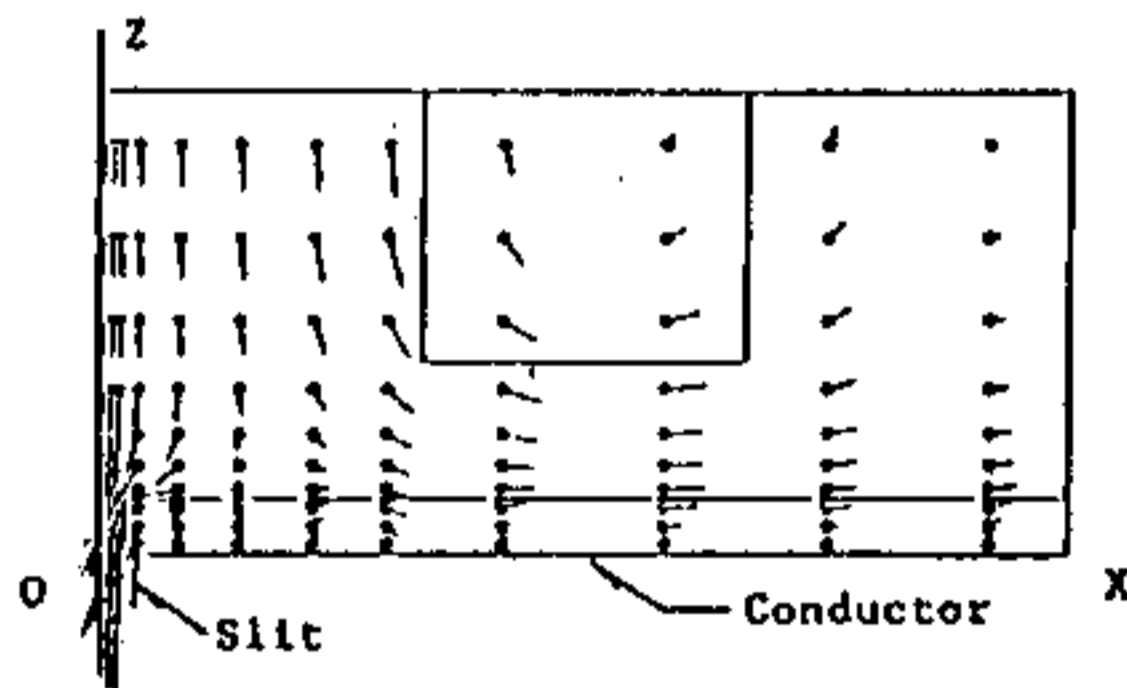


Fig.4 Flux Density Distribution
(a) Y-Z Plane
(b) X-Z Plane



ROLE OF SCALAR POTENTIAL

Fig.5 shows the real part distribution of the scalar potentials calculated on the top surface of the right hand copper plate. The line E-F shows the transverse line in the center, while the line A-E shows the side adjacent to the slit. Scalar potentials along the line A-E appear larger than those along the line B-F.

To study the role of the scalar potential, the expression of the eddy current density is restated as

$$\vec{J}_e = -j\omega\vec{A} - \sigma\text{grad } \phi$$

The first term indicates the component by the vector potential, while the second term is the component by the gradient of the scalar potential. If we don't take ϕ into account, the calculation results show that eddy currents flow in opposite direction to the route of the impressed currents. Because the direction of the vector potential \vec{A} is decided mainly by the impressed currents. The above fact means there exist eddy currents perpendicular to the boundary A-E adjacent to the air-slit in our model. Such flow of eddy currents is physically impossible. In the next place, when we consider the scalar potential, the results show that the second component of the eddy current cancels the flow perpendicular to the boundary A-E, so that eddy currents turn to circulate in the conductor. The inference from the above calculated results of our

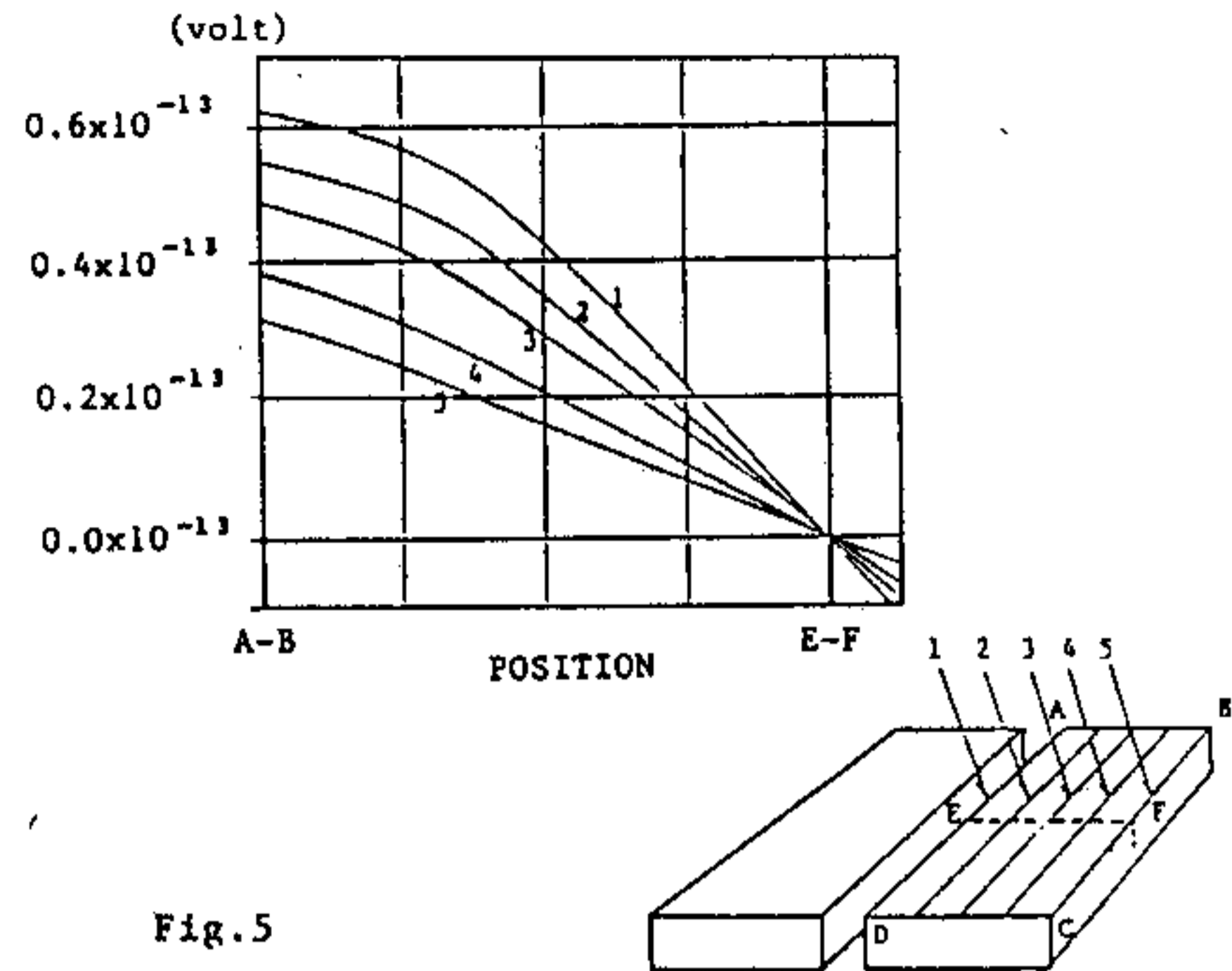


Fig.5 Scalar Potential Distribution
(for 2.0×10^{-12} AT/mm²)

model, shows that the scalar potential must be taken into consideration when we treat a model including conductors with any discontinuity or any gaps in the stream-lines similar to the flow of the impressed currents. In such a model the scalar potential works to compensate the incomplete expression of the eddy current density by the vector potential \vec{A} only.

CONCLUSION

A fundamental model of our flux concentration apparatus is analyzed by applying our newly developed iterative method. The intensification of the magnetic flux in the air-slit and its reflection on a conductor plate are sought and confirmed visually. Comparison of the flux density with the measured values shows close resemblance.

As for the role of the scalar potential, we have concluded from the real analysis of our model that the scalar potential is necessary when we treat such a model including conductors with any discontinuity or any gaps in the stream-lines similar to the flow of the impressed currents.

REFERENCES

- [1] T.Yoshimoto et al., "3-D Finite Element Analysis of Flux Reflection and Flux Concentration Effects of Eddy Currents," IEEE Trans. on Magnetics, Vol.MAG-22, No5, 1986.
- [2] K.Bessho et al., "Asymmetrical Eddy Currents and Concentration Effect of Magnetic Flux in a High Speed Rotating Disc," IEEE Trans. on Magnetics, Vol.MAG-21, No5 1985.
- [3] M.V.K.Chari et al., "Three Dimensional Vector Potential Analysis for Magnetic Field Problems," IEEE Trans. on Magnetics, Vol.MAG-18 No2 1982.
- [4] S.J.Salon et al., "Three Dimensional Eddy Currents Using a Four Component Formulation," IEEE Trans. on Magnetics, Vol.Mag-20 No-5, 1984.
- [5] C.S.Biddlecombe et al., "Methods for Eddy Current Computation in Three Dimensions," IEEE Trans. on Magnetics, Vol.MAG-18 No2 1982.
- [6] M.V.K.Chari et al., "Three Component Two Dimensional Analysis of the Eddy Current Diffusion Problem," IEEE Trans. on Magnetics, Vol.MAG-20 No5 1984.
- [7] W.Müller et al., "A Method for Numerical Calculation of 3-D Eddy Currents," IEEE Trans. on Magnetics Vol.Mag-21 No6 1985.
- [8] O.C.Zienkiewicz, The Finite Element Method in Engineering Science, McGraw-Hill Publishing, 1971.